Proceedings of the 26th International Conference on Offshore Mechanics and Arctic Engineering
OMAE2007
June 10-15, 2007, San Diego, California, USA

OMAE2007-29562

PHENOMENA OBSERVED IN VIV BARE RISER FIELD TESTS

Hayden Marcollo
hayden_marcollo@amogconsulting.com
AMOG Consulting

Hemant Chaurasia
hemant_chaurasia@amogconsulting.com
AMOG Consulting

J. Kim Vandiver
kimv@mit.edu
Department of Mechanical Engineering
Massachusetts Institute of Technology

ABSTRACT

The following paper presents the results of preliminary data analysis performed on a densely instrumented bare riser undergoing Vortex-Induced Vibration (VIV) response at high mode number. The data analysis steps are presented and show a method whereby it is possible to resolve uncertainty in the orientation of strain gauges on a riser responding to VIV. Two new phenomena are then revealed from the data analysis. The first is the occurrence of higher harmonic VIV response in directions which are not orthogonal to the cross-flow and in-line directions. Secondly, evidence of riser structural response in the form of wave propagation is observed.

INTRODUCTION

The Vortex-Induced Vibration behavior of offshore risers at predicted high mode numbers (>20) is becoming an area of great interest as the offshore industry conducts exploration and production activities in ever deeper waters, where drilling and production risers become longer and the response occurs at higher mode numbers. The increased interest is also due to the results from first round offshore VIV field tests conducted in 2004, termed “Miami1” and funded by DEEPSTAR [2]. The data revealed very large contributions to fatigue damage due to the presence of higher harmonics. As a follow-up testing program, DEEPSTAR funded another set of offshore field tests termed “Miami2”.

The Miami2 tests were conducted in late 2006 and their aim was to:

- Gather a rich data set of differential strain measurements in uniform to highly sheared flow conditions.
- Test the VIV response of different fairing and strake configurations.

The tests achieved both objectives. The rich set of differential strain measurements is the subject of this paper, together with the results of a preliminary data analysis conducted on it. This paper is structured as follows:

- Description of experiments
- Data and data processing
- Phenomena observed

DESCRIPTION OF EXPERIMENTS

The Miami2 experiments are discussed in [4], [5] and [6]. The experiments involve a vertically towed riser suspended from a vessel, with a railroad wheel used as a bottom weight. The riser properties are shown in Table 1.

Table 1 –Gulf Stream Miami2 (2006) Riser Properties

Inner Diameter	0.98 in (0.02489 m)
Outer Diameter	1.43 in (0.03632 m)
Optical Fiber Diameter	1.30 in (0.033 m)
EI	2.14×10^5 lb.in^2 (613 Nm^2)
EA	1.33×10^6 lb/ in^2 (9.21×10^9 N/m^2)
Weight in Seawater	0.133 lb/ft (flooded in seawater) (1.942 N/m)
Weight in air, w/trapped water	0.511 lb/ft (7.46 N/m)
Effective Tension	725 lbs submg. bottom weight
Material	Fiberglass with epoxy
Length	500.4 ft (152.4m) U-Joint to U-Joint

Important parameters of the tests are summarized in Table 2 by stating what the limits of these parameters were.

Table 2: Important parameters limits of tests

Max. velocity	~ 4 ft/s
Max. Strouhal frequency (St=0.20)	~ 7 Hz
Minimum wavelength associated with max speed	~ 14 ft
Maximum predicted mode number	~ Mode 40
Max. top angle of riser to the vertical	~ 65 degrees
Max *Re* number	~ $3x10^4$

The experimental measurement system was carefully optimized in the design process to resolve both maximum spatial and maximum temporal information from the tests within a bandwidth limit constraint. Of importance with the temporal information is resolving the higher harmonics of VIV, and of importance in the spatial information is being able to resolve the smallest wavelengths (either traveling or standing waves) that respond to the Strouhal frequency excitation.

Measurement system

The measurement system consisted of:

- Fiber optic strain gauges
- Load cell & tilt meter
- ADCP and mechanical current meters

The test riser used in the Miami2 experiments was instrumented by 8 embedded optical fibers, grouped in pairs at four equally spaced locations around the circumference of the riser, producing strain time series information. Each fiber contained 35 strain gauges mounted roughly 14 feet apart in a staggered arrangement such that in any given quadrant of the riser, there was a strain gauge every 7 feet along the length of the riser. In the analysis here only the odd numbered fibers are used to determine differential bending strain at 14 ft intervals, due to a synchronization problem with one of the even fibers that is yet to be resolved. The strain data was typically sampled at 50.4857 Hz and test durations were typically 180 seconds. Average values reported in this paper are for the duration of each three minute test.

A load cell and tilt meter were mounted at the top of the riser to provide time series information on the static and dynamic behavior at the top of the riser during the tests.

The current profile was measured using an Acoustic Doppler Current Profiler (ADCP), which returned current speed and direction as a function of depth in a series of frequently occurring "pings". These pings were averaged to obtain an average current profile relative to the boat for the duration of each test. The ADCP data was cross-checked with the readings from mechanical current meters, which showed good agreement. The premise that the current profile *normal to the riser* is the one that drives the VIV phenomena was adopted, and a process for determining the normal current was used that has been previously described in [3].

DATA AND DATA PROCESSING

Strain time series information obtained from each test was converted into differential bending strain by differencing diametrically opposed gauges. Two orthogonal planes of bending strain were then determined at each axial location of the sensor group as follows:

$$X(z,t) = Q1(z,t) - Q3(z,t);$$
$$Y(z,t) = Q2(z,t) - Q4(z,t);$$

Where X and Y are the orthogonal differential bending strains from the respective quadrants [*Q1,Q3*] and [*Q2,Q4*] at a position z along the riser's length at time t. Note that only data from the odd number fibers was used in this exercise.

Unwrapping the data

The fiber optic strain gauges running axially in the pipe were discovered to have a residual 180° twist over the length of the pipe (a by-product of the manufacturing process). The twist was a global twist in all fibers, such that at any location z the four pairs of fibers were still 90° apart in orientation. Computing the cross-flow and in-line components of riser bending strain (by differencing 1st and 3rd quadrants and 2nd and 4th quadrants respectively) was only possible by performing an instantaneous vector rotation on the data to resolve the true components. The following algorithm was used to compute true cross-flow and in-line bending strains (X' and Y' respectively) from raw differential strains (X and Y):

$$X' = X\cos(\theta) + Y\sin(\theta)$$
$$Y' = -X\sin(\theta) + Y\cos(\theta)$$

Here, θ is the angle by which the Q1-Q3 plane must be rotated in order to line up with the true cross-flow direction.

To compensate for the twist, initial attempts were made with a vector rotation linearly increasing between 0° and 180° over the riser length; however after trying this, it was evident from the time series and frequency content that this assumption was incorrect. The precise amount of twist in the pipe at each sensor's location had to be uniquely determined.

The unique angle of twist at each sensor location was found from the premise that true cross-flow vibrations should have spectral peaks only at the Strouhal frequency and *odd* multiples of this. In contrast, in-line vibrations will exhibit spectral peaks only at *even* multiples of the Strouhal frequency, with a minimum at the Strouhal frequency itself. Hence, it should be possible to deduce the unique angle of twist for each sensor location by vector-rotating the corresponding set of Q1-3 differential strain data until the PSD shows a maximum value at the Strouhal frequency.

The towing test selected for this exercise was a particularly uniform and unidirectional flow test. At every sensor position along the riser, the data was vector-rotated in turn through every angle between 0° and 360° (in 1° increments), and at each angle of rotation, the PSD of the rotated Q1-3 differential strain was measured. The PSD in a narrow band around the Strouhal frequency was the important measurement, as this would be a maximum value at the angle which correctly rotated the Q1-3 plane into the cross-flow direction.

The results of this analysis are presented in Figure 2 (see Annex A), using quadrant strain time series data for the latter 60 seconds of Miami 2 test run 20061023203818 (chosen for its particularly well-behaved steady state vibration, and well-defined harmonic peaks in its PSD as referenced in [5]). This figure shows the PSD of rotated differential strain in a band around the fundamental Strouhal frequency, for all possible rotation angles. The horizontal axis is the rotation angle, the vertical axis is the location down the pipe, and the color represents the intensity of the PSD. The picture on the left represents the orientation of the actual plane of the Q1-Q3 fibers. The twist in the riser is evident from the locations of the peaks in the PSD; at the top of the riser there is very little twist and the Q1-3 plane is well aligned with the cross-flow direction, but further down the riser there is a region of sudden twist followed by a more gradual twist to the bottom, accumulating a total twist of 180° to the bottom of the riser (as found in the manufacturing process). Note that there are practical issues that made it infeasible to calibrate the coil tubing twist on land.

Using these twist results, the unique angle of rotation required at each sensor location was measured and was thereafter used to "unwrap" the differential strain data (for both Q1-3 and Q2-4) for every Miami 2 test considered.

PHENOMENA OBSERVED

Observed frequency content of VIV

Vector rotations were also performed on the unfiltered data to examine the occurrence of the higher harmonics. The presence of higher harmonics (harmonics of the Strouhal frequency) were observed in these high mode number experiments and are also discussed in [2]. The frequency content is shown in Figure 1 as a function of the orientation around the riser, by carrying out a vector rotation around the riser. The horizontal axis corresponds to the angle of orientation, and the vertical axis is frequency. The color represents magnitude of the PSD.

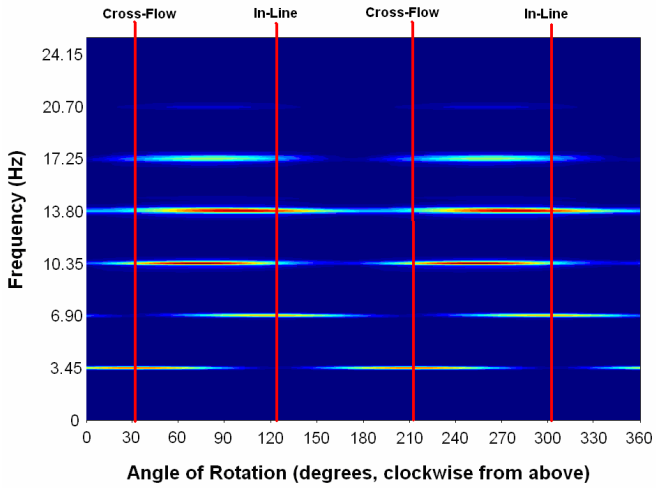

Figure 1: The occurrence of higher harmonics are confirmed and observed not to line up with cross-flow or in-line directions; color represents magnitude of the PSD.

Figure 1 shows that, around a full circle of 360°, there are two maxima of 1st harmonic and 2 orthogonal maxima of the 2nd harmonic, which correspond to the cross-flow and in-line planes of vibration respectively. The frequencies higher than 6.90 Hz correspond to the 3rd, 4th, 5th and 6th harmonics, and it can be observed that their maxima do not line up in the same directions as the cross-flow and in-line.

In the past, limited attention has been given to the orientation of occurrence of higher harmonics. It has previously been commented [2] [9] that the odd harmonics line up in the cross-flow direction while the even harmonics line up in the in-line direction. Calculations reported in these references have used the spectra at specific orientations hence taking into account the real contributions to fatigue at these orientations.

One explanation for the higher harmonics not lining up is that the "2T" vortices [8], which have been hypothesized in [5] as being the cause of the higher harmonics, apply an asymmetric dynamic force on the riser that is neither exclusively cross-flow nor in-line in direction.

RMS response

A physical understanding of the VIV response of the riser was sought by focusing on the cross-flow Strouhal frequency excitation.

The cross-flow RMS stress and fatigue damage response of the riser was calculated. Stress amplitude was calculated from the differential bending strain as follows:

$$\sigma_{bX',Amp} = E\frac{X'}{2}$$

Where $\sigma_{bX',Amp}$ is the stress amplitude in the *X*' plane, *E* is the Young's modulus of the material and *X'* is the differential bending strain amplitude (peak to peak).

Fatigue was calculated using the rainflow method of counting the time series. The S-N data parameters used were API-X' parameters, which correspond to use in offshore risers at weld locations. Parameters given as input to the WAFO program [1] were Gamma = 5.3424×10^{-13} (for Stress Amplitudes in units MPa – note, this is for amplitudes *not* ranges) and Beta = 3.74. The 1st harmonic cross-flow time series data was used to determine all RMS stress averages, and for all rainflow counting operations on the data. There were no contributions from in-line response or higher harmonics included in this calculation.

The cross-flow RMS stress and fatigue response is shown along the riser in Annex A, Figure 3 for a particularly stationary (steady-state) test. It is not known what the cause of the peak in bending stress occurring at x/L = 0.8 is due to; perhaps a bad gauge; when converted to fatigue damage its effect is reduced as the cross-flow 1st harmonic frequency increases down the pipe.

Both the RMS bending stress and fatigue are observed to decay near the bottom end despite the high current velocities normal to the riser, which are shown on the left hand side. Occasionally in the data some dropouts from the furthest gauges are observed however the decay occurs consistently in all the Miami2 data for both the rms response from a single gauge as well as the differential response. This decay effect is contrary to intuition where there would be an expectation that standing wave structural response of the riser should produce antinodes with the largest curvature and stress at the bottom, given the strongest current velocity normal to the riser.

Time history response

A strain time history plot of cross-flow 1st harmonic bending strain along the length of the riser was constructed to gain a greater physical understanding of the VIV response. The plot is shown in Annex A, Figure 4. The intensity of the color indicates the value of bending strain (peaks in curvature at antinodes). The vertical axis is the pipe axis (top to bottom) and the horizontal axis is time.

The plot is very revealing due to the high spatial density of gauges. It shows evidence that the majority of the riser has a propagating bending wave, exhibited in the diagonally striped pattern. This plot is typical of all Miami2 bare riser data plotted to date.

At the lower region of the riser, in the proximity of the railroad wheel connection, the propagating response is shown to become disrupted. At this lower location there is also some evidence of a standing wave response pattern where it can be seen that some antinodes are occurring simultaneously. The standing wave response pattern is presumably due to reflections from the bottom end.

Clearly, if the riser is responding in a traveling wave mode, then the vortices being shed along the length are not shed in phase with the vortices up and down the riser.

The decay in response near the boundary seems to be due to the dominant traveling mode being disrupted by the standing wave behavior near the boundary.

To examine the propagation in more detail, a theoretical calculation for the speed was made.

Wave propagation theory

If a 'cable' or 'string' system is considered where the effects of bending stiffness, *EI,* are neglected, then the instantaneous propagation speed of a transverse wave is given by *c*:

$$c = \sqrt{\frac{T}{m_L}}$$

where: c = speed of traveling wave;
T = tension in riser;
m_L = inertial mass per unit length of riser.

The riser used in the tests reported in this paper had very little contribution from *EI* and very little variation in tension along its axis, such that the above expression can be used as a good approximation.

The parameter m_L is the inertial mass per unit length and includes both the mass of the riser and its contents, as well as the added mass as shown by the following equation:

$$m_L = m_{a,filled} + \rho_\omega Ca \frac{\pi D_o^{\,2}}{4}$$

where: $m_{a,filled}$ = mass of riser in air and contents;
ρ_ω = density of water, or other surrounding fluid;
Ca = added mass coefficient;
D_o = outer-diameter of riser.

The tension measured in the experiments, primarily due to the submerged weight of the rail road wheel, was T = 720 lbs. From Table 1, m_L = 0.511 lb/ft. Assuming Ca = 1, then the theoretical wave propagation speed of transverse bending waves is:

$$c = 137 \text{ ft/s.}$$

This calculated speed is close to the observed wave propagation speed of 130 ft/s as shown on Figure 4, which provides greater evidence that wave propagation is occurring.

One of the important next steps in understanding VIV response under wave propagation conditions is to determine amplitudes of the propagating waves, as this directly affects the stress and fatigue.

SUMMARY AND RECOMMENDATIONS

A data analysis method is demonstrated whereby the orientation of the strain gauges of a riser undergoing VIV can be determined without prior knowledge.

The occurrences of higher harmonics are observed to not line-up with cross-flow and in-line directions. It is important to be aware of this effect when attempting to make any empirical estimation of the effects of higher harmonics.

Evidence of riser structural response in the form of wave propagation is observed to govern the response. At preliminary stage it appears that the wave propagation speed behaves close to the predictions of simple theory. Understanding the physics of the propagation is an important next step including when do end effects matter and what is the behavior of amplitude and amplitude decay rate.

NOMENCLATURE

E	Young's Modulus
I	Moment of Inertia
D	Diameter
X	differential strain from quadrants 1 and 3
Y	differential strain from quadrants 2 and 4
X'	cross-flow bending strain
Y'	in-line bending strain
c	wave propagation speed
$m_{a,filled}$	mass of riser in air and contents
ρ_ω	density of water/surrounding fluid
Ca	added mass coefficient
D_o	outside diameter
T	tension
t	time
m_L	mass per unit length
θ	rotation angle

ACKNOWLEDGMENTS

DEEPSTAR and DEEPSTAR personnel for funding and assisting on field trip. The crew of the Walton Smith , University of Miami, for providing valuable assistance and support. MIT students Susan Swithenbank, Vikas Jhingran and Vivek Jaiswal for their data analysis assistance. Insensys and Fiberspar personnel for their efforts in fabricating the riser and instrumentation system.

REFERENCES

[1] Wave Analysis for Fatigue and Oceanography. Homepage, Lund Institute of Technology, March 2007, http://www.maths.lth.se/matstat/wafo/

[2] Vandiver, J.K., Swithenbank, S.B., Jaiswal, V. and Jhingran V., 2006, "Fatigue damage from high mode number vortex-induced vibration", Proceedings of OMAE2006, OMAE2006-9240

[3] Vandiver, J.K., Marcollo, H., Swithenbank, S. and Jhingran, V., 2005, "High Mode Number Vortex-Induced Vibration Field Experiments". Offshore Technology Conference OTC 17383

[4] Swithenbank, S. and Vandiver, J.K., 2007, "Identifying the Power-in Region for Vortex-Induced Vibration on Long Flexible Cylinders", Proceedings of OMAE2007, OMAE2007-29156

[5] Jhingran, V. and Vandiver, J.K., 2007, "Incorporating the Higher Harmonics in VIV Fatigue Predictions", Proceedings of OMAE2007, OMAE2007-29352

[6] Jaiswal, V. and Vandiver, J.K., 2007, "VIV Response Prediction for Long Risers with Variable Damping", Proceedings of OMAE2007, OMAE2007-29353

[7] Blevins, R.D., 2001, Flow-Induced Vibration, Krieger Publishing Company

[8] Jauvtis, N. and Williamson, C.H.K., 2004, "The effect of two degrees of freedom on vortex-induced vibration at low mass ratio", Journal of Fluid Mechanics, 509:23-62

[9] Vandiver, J.K., Swithenbank, S., Jaiswal, V. and Marcollo, H. 2006, "The Effectiveness of Helical Strakes in the Suppression of High-Mode-Number VIV", OTC 18276.

ANNEX A

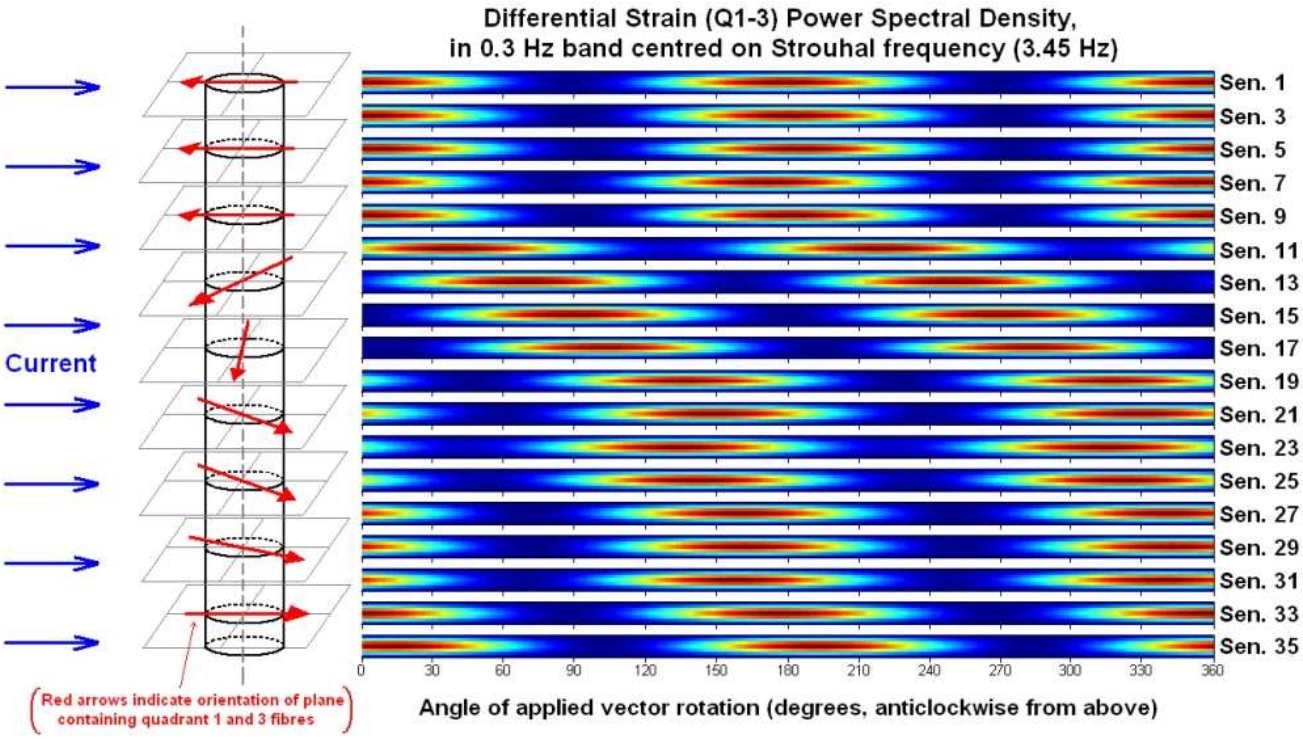

Figure 2: Illustration of determining twist along the riser by maxima in the cross-flow Strouhal response

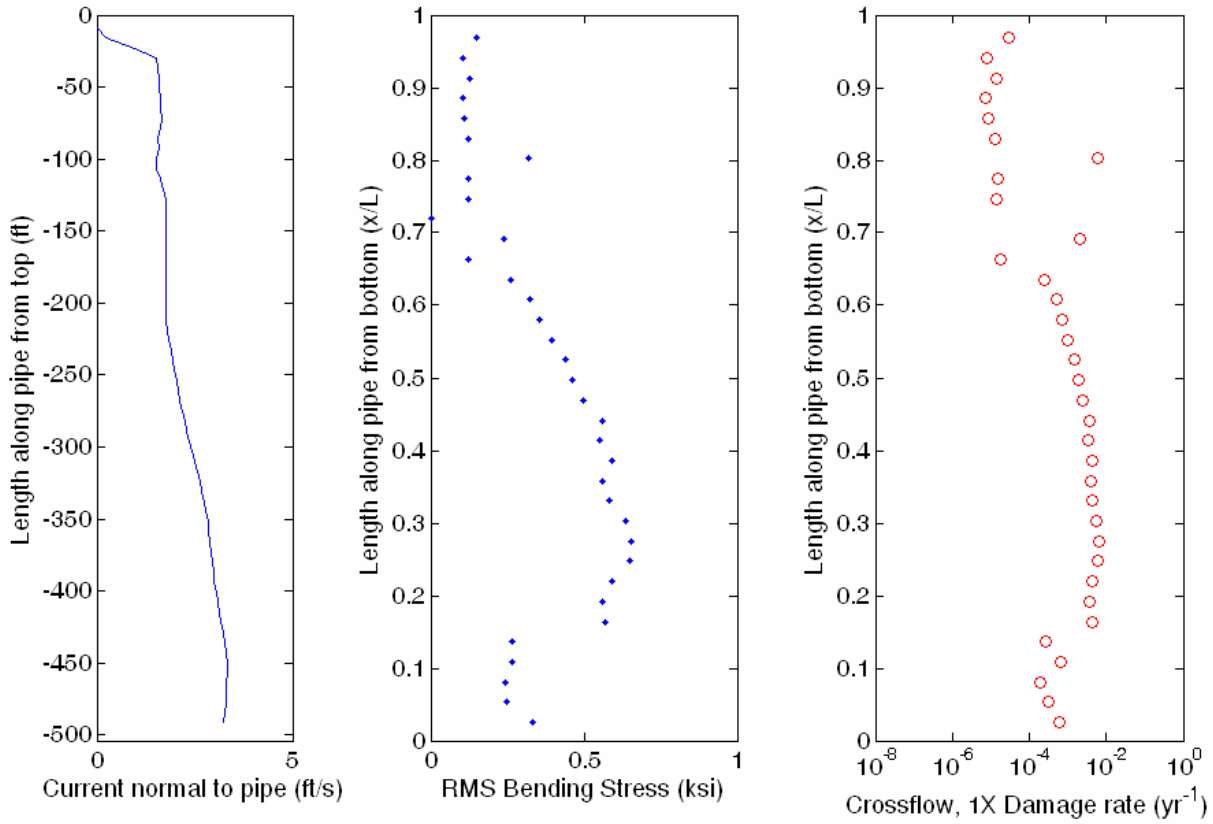

Figure 3: RMS response from a relatively steady state test

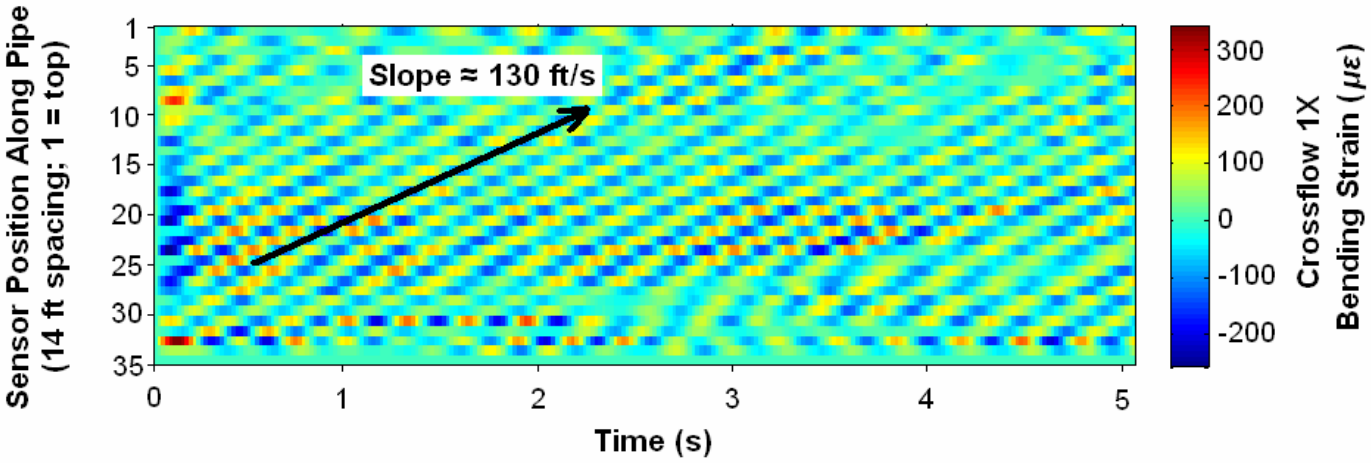

Figure 4: Evidence of VIV response in the form of wave propagation